

Electrically Switchable Graphene Photo-Sensor using Phase-Change Gate Filter for Non-Volatile Data Storage Application with High-Speed Data Writing and Access

Gang Zhang, Tian-Zi Shen, Hua-Min Li, Dae-Yeong Lee, Chang-Ho Ra, and Won Jong Yoo *

Sungkyunkwan University, Samsung - SKKU Graphene Center (SSGC), Suwon, Gyeonggi-do, 440-746, Korea

* Phone: 82-31-290-7468, Fax: 82-31-299-4119, Email: yoowj@skku.edu

ABSTRACT

An electrically switchable graphene photo-sensor (SGPS) is proposed for multiple functional applications. SGPS is a dual-gate thin-film transistor with a graphene channel and a phase-change chalcogenide (GeSbTe) gate filter. This gate filter is switchable between the amorphous (optically transparent) and crystalline (optically non-transparent) phases by applying the gate biases. When the gate filter is switched to the amorphous /crystalline (*a/c*) phases, the SGPS will/not yield photo-current (I_{pc}) under a constant light source. By detecting the presence of I_{pc} , two data states can be read out so as to accomplish non-volatile data storage. SGPS can present a switching speed of ~50 ns between the *a/c* phases of GeSbTe and a data access speed as fast as 10 ns. SGPS shows very good 10-year data retention at 85°C and good endurance of >10⁶ switching cycles between the *a/c* phases of the GeSbTe gate filter.

INTRODUCTION

Graphene is regarded as an interesting candidate material for future solid-state devices applications [1-5]. Graphene has excellent mechanical property and thermal conductivity, large carrier mobility (~2×10⁵ cm²/Vs) with about zero band-gap [3]. When graphene is adopted for photo-detection, very-fast response speed (>50GHz) and broad wavelength range (far IR to UV) can be obtained [3]. By introducing a switchable gate (optical) filter for the graphene photo-sensors, as illustrated in Fig. 1(a), the presence of I_{pc} under a constant light source is determined by the optical transmittance of the gate filter. For example, when the GeSbTe gate filter is at the *a* phase, the incident light (with proper wavelength) can penetrate the gate filter and generate I_{pc} in the bending junctions of the graphene channel. In contrast, when the gate filter is at the *c* phase, the same incident light is reflected and little I_{pc} can be generated, as shown in Fig. 1(b). As a result, the drain current (I_d) read at a constant light source is only determined by the phases of the gate filter, as shown in Fig. 1(c).

As the optical transmittance of the GeSbTe gate filter is determined by its *a/c* phase states, which are non-volatile and electrically switchable [6-8], the GeSbTe gate filter can be programmed/erased to stable *a/c* phases by proper gate biases, as shown in Fig. 2. The gate filter at the *a/c* phases will/not yield stable data readout (I_{pc}) under a constant light source, as shown in Fig. 3. Note that in SGPS, the gate filter stores data information according to two photo transmittances, while the graphene photo-sensor reads out these two data states.

SGPS may be adopted for multiple applications, *i.e.*, smart photo-sensors, non-volatile data storage, and embedded logic system (when a constant light source is provided). When used for non-volatile data storage, SGPS may show very fast write/read speed as compared to Flash and the other emerging non-volatile memories, as shown in Table 2.

(Dr. Zhang Gang was with the SSGC until July, 2011. He is with Samsung Electronics, Hwasung, Korea, since August, 2011)

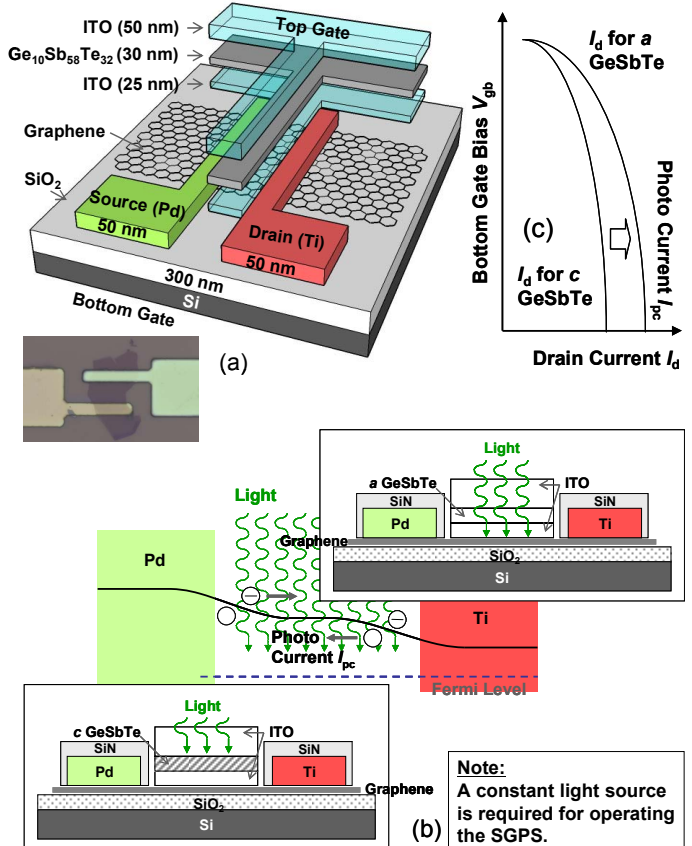


Fig. 1: (a) Illustration of the device structure of the SGPS. The ITO/GeSbTe/ITO gate filter is added for a graphene photo-sensor, whose image is shown in the inset. The distance between the Pd and Ti electrodes is 1 μ m. (b) Energy band diagram of the SGPS. With light illumination, photo current I_{pc} is obtained at the bending junctions of the graphene channel. Without light illumination, no I_{pc} is obtained. (c) Illustration of the I_d - V_{gb} transients with/out I_{pc} for the graphene photo-sensor. (Note that I_d rises at negative V_{gb} [3])

DEVICE DESIGN AND EXPERIMENT

The device structure of SGPS is shown in Fig. 1. A SGPS cell has a 25/30/50-nm-thick ITO/GeSbTe/ITO top gate filter, in which the top ITO is the top gate electrode and the bottom ITO passivates GeSbTe and the graphene channel. SGPS is fabricated as followings: (i) single-layer graphene (HOPG in this study) was transferred to 300-nm-thick SiO₂/Si wafer; (ii) Pd/Ti (as source/drain electrodes) were formed by sputtering; (iii) SiN barrier was deposited by CVD on Pd/Ti; (iv) top gate filter was formed by sputtering. Photolithography was used in this study for the graphene photo-sensor fabrication.

The GeSbTe deposited by co-sputtering has a composition of Ge₁₀Sb₅₈Te₃₂ in atomic percent. AFM image of a reference GeSbTe film (30-nm-thick) is shown in the inset of Fig. 4(a). Electric phase switch characteristics of a reference film of 30-nm-thick and 150 × 150 nm² patterned are shown in Fig. 4(a).

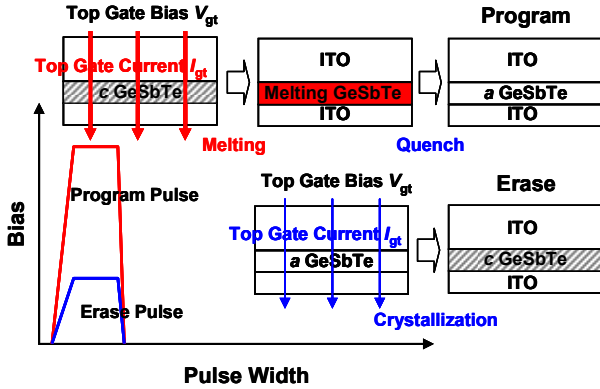


Fig. 2: Illustration of phase switching processes of a $\text{Ge}_{10}\text{Sb}_{58}\text{Te}_{32}$ film embedded in ITO conducted by electric bias. When a large bias is applied, the GeSbTe film melts due to Joule heating and ends up at an amorphous (*a*) phase after quenching; when a low bias is applied, the GeSbTe film changes its phase from *a* to crystalline (*c*) to attain a thermodynamic equilibrium. Remarkably, the photo transmittances of the GeSbTe film vary depending on the *a/c* phases [6].

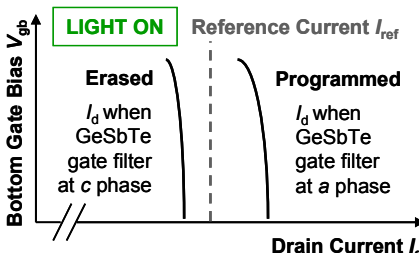


Fig. 3: Illustration of the I_d - V_{gb} transients when the SGPS is under a light illumination but the gate filter is at the *a/c* phases. The readout I_d rises by the amplitude of I_{pc} when the gate filter is at the *a* phase. In contrast, the readout I_d has no such increase when the gate filter is at the *c* phase. If I_{pc} is large, *i.e.*, a few μA , a reference current (I_{ref}) may be introduced to read out two stable data states so as to enable data storage. We define the *a/c* phases to be the programmed/erased states in this study.

It is suggested that the top gate current density (J_{gt}) may need to be larger than $1.07 \times 10^{-7} \text{ A}/\text{nm}^2$ with a 2/50/2 ns waveform so as to program (from the *c* phase to the *a* phase) a SGPS cell. The large J_{gt} is required for melting the crystalline GeSbTe by Joule heating. The melting GeSbTe will end up at the *a* phase after quenching. In this manner, the SGPS is programmed (see Fig. 2). The *a* phase of the GeSbTe is thermodynamically not equilibrium, and it tends to change to the *c* phase of GeSbTe. A smaller J_{gt} can lead to the phase change from *a* to *c* so as to erase the SGPS (see Fig. 2). Note that the top gate current I_{gt} required for programming a SGPS cell may be proportional to the area of the gate filter (s_{gt}) as $I_{gt} = J_{gt} \times s_{gt}$. Thus, the I_{gt} for programming may be very large when the s_{gt} is large, *i.e.*, $I_{gt} = \sim 0.24 \text{ mA}$ when $s_{gt} = \sim 0.25 \mu\text{m}^2$ in this study. However, we think that the scaling of s_{gt} must effectively reduce the I_{gt} for the SGPS. On the other hand, the scalability of the SGPS is determined by the junction area of the graphene channel [3]. Such *a/c* phases switching is endurable over no less than 10^6 cycles, as shown in Fig. 4(b). It has been reported that GeSbTe shows the cycling endurance between the *a/c* phases of 10^{11} - 10^{12} cycles when GeSbTe is used for phase-change random-access memory (PRAM) applications [6-8]. We think that the SGPS using the same GeSbTe material shall show similar cycling endurance to the PRAM.

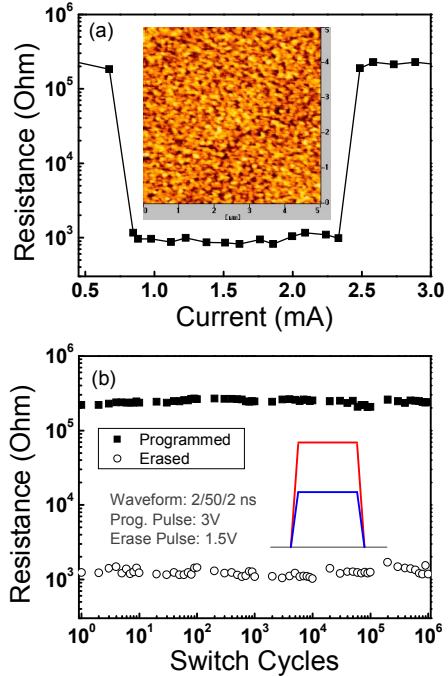


Fig. 4: (a) Electric characteristics of the phase switches of a reference GeSbTe film (30-nm-thick, $150 \times 150 \text{ nm}^2$ patterned). Inset shows the AFM image of the reference film at the (poly-) crystalline phase. (b) The electric characteristics of 10^6 phase switching cycles conducted by 3V/1.5V switching biases applied for 2/50/2 ns.

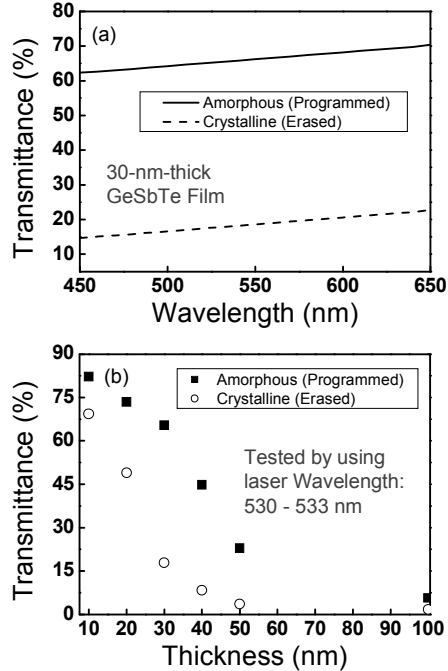


Fig. 5(a) shows the photo transmittance transients of the 30-nm-thick reference GeSbTe film at the *a/c* phases. The tested GeSbTe film shows clear difference in optical transmittances at the *a/c* phases. For example, the optical transmittance is $\sim 65\%$ at the *a* phase while it is $\sim 17\%$ at the *c* phase when the incident light

Fig. 5(a) shows the photo transmittance of the 30-nm-thick reference GeSbTe film at the *a/c* phases. The tested GeSbTe film shows clear difference in optical transmittances at the *a/c* phases. For example, the optical transmittance is $\sim 65\%$ at the *a* phase while it is $\sim 17\%$ at the *c* phase when the incident light

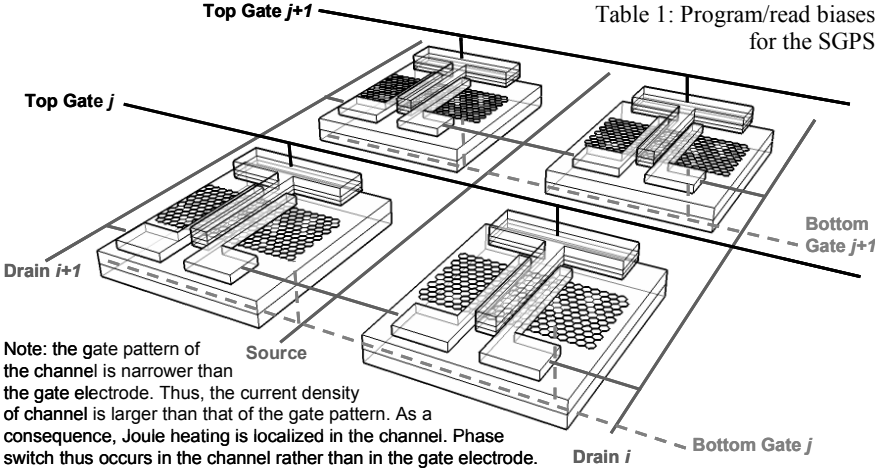


Table 1: Program/read biases for the SGPS

	Bias	Condition
Program		
A selected cell	$V_{gt} + V_d $ (4V)	Melting-quench
Cells share V_d	$-V_d$ (-1V)	No melting
Cells share V_{gt}	V_{gt} (3V)	No melting
Read		
A selected cell	V_{gb} and V_d	I_{pc} is readable
Cells share V_d	V_d (0.3V)	No I_{pc}
Cells share V_{gb}	V_{gb} (-25V)	No I_{pc}

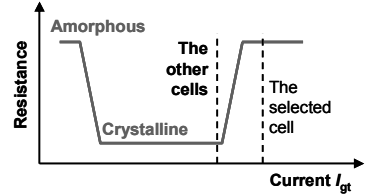


Fig. 6: Illustration of a possible circuit design for the SGPS when it is used for data storage. The GSPS cells may share the same source/drain lines in a column and the same top/bottom gate lines in rows with the other cells. When a random GSPS cell is selected for program, top gate bias (V_{gt}) as well as negative drain bias ($-V_d$) are applied to it for program. The other cells are biased by only V_g or $|V_d|$, which is insufficient to program these cells, as shown in the illustration in the right side. Similarly, bottom gate bias (V_{gb}) and V_d are applied to read a random cell. The other cells are not read as no I_{pc} is detected. The possible bias conditions for programming and reading a GSPS cell is shown in Table 1.

has the power of $\sim 1\text{mW}$ and the light wavelength of $\sim 530\text{ nm}$. Fig. 5(b) shows the photo transmittances of the GeSbTe films with the thicknesses of 10 - 100 nm. We think that the 30-nm-thick film provides a proper photo transmittance: A thicker film shows too small transmittance at the *a* phase, while a thinner film shows very large transmittance at the *c* phase.

When the SGPS is used for non-volatile data storage, SGPS can be integrated in NOR-type circuits for random access and writing, as shown in Fig. 6. The top gate (V_{gt}) and drain (V_d) biases are applied so as to program a random cell; the bottom gate bias (V_{gb}) and V_d are applied to read a random cell; Array /block erase is required for this circuit, as shown in Table 1. It is noted that V_{gb} is used for data read in this study to avoid the disturbance induced by the variations of top gate resistances.

PHOTO-SENSOR PERFORMANCE

Fig. 7(a) shows the I_d - V_{gb} characteristics of the SGPS cell when the gate filter is at the *a/c* phases. It is found that the I_d is increased by $\sim 3\mu\text{A}$ when $V_{gb} = -25\text{V}$ and the gate filter is at the *a* phase. The light source applied for this experiment has the power of $\sim 1\text{mW}$ and the wavelength of $\sim 530\text{ nm}$. We think that the I_d increase is due to the generation of I_{pc} , and the I_{pc} of $\sim 3\mu\text{A}$ may provide a clear margin for data read (see Fig. 3). In contrast, no I_d increase (I_{pc}) is observed when the gate filter is at the *c* phase under the same light source. In this manner, two stable data states can be read out so as to accomplish non-volatile data storage and access.

Fig. 7(b) shows the I_{pc} characteristics at the read frequency of 10^8Hz . Clear data readout is obtained when the $V_{gb} = -25\text{V}$ with the waveform of $1/8/1\text{ ns}$ is applied and the gate filter is at the *a* phase. It has been reported that the graphene field-effect transistor can present very fast access speed due to the very high carrier mobility in the graphene channel [1-3]. We think that the SGPS may fully adopt the device property of the graphene field-effect transistors. Thus, it is expected that the SGPS may show an access speed of 50 - 100GHz . This makes the SGPS an interesting candidate for the high-speed working memory applications. In contrast, the other non-volatile memories in Table 2 may be unable to show such a high frequency access speed partially due to their smaller carrier mobilities in the resistors and the selectors [9].

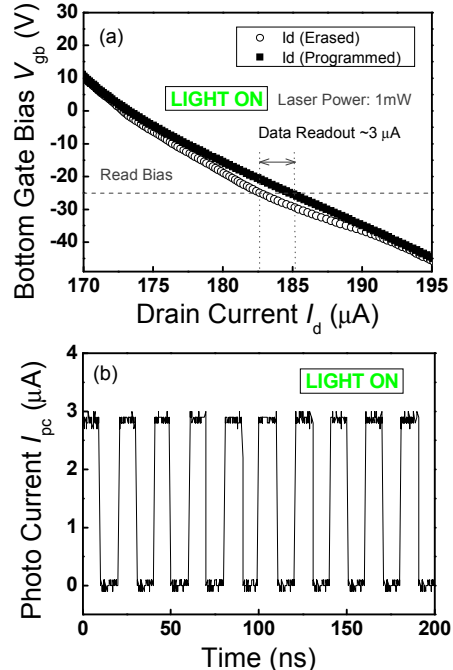


Fig. 7: (a) I_d - V_{gb} characteristics of the proposed SGPS under the light illumination (wavelength of $\sim 530\text{ nm}$, power of 1mW) when the gate filter is at the *a/c* phases. I_{pc} of $\sim 3\mu\text{A}$ is detected at $V_{gb} = -25\text{V}$ and $V_d = 0.3\text{V}$. (b) The I_{pc} characteristics of the SGPS (gate filter is at the *a* phase) read by V_{gb} of -25V with the waveform of $1/8/1\text{ ns}$.

The SGPS also shows very fast program/erase speed of no more than $2/50/2\text{ ns}$ (see Fig. 4). Meanwhile, SGPS has good compatibility with the graphene field-effect transistors in the process technologies. Thus, we think that the SGPS can be a very promising concept for the graphene-based logic systems applications. Nevertheless, SGPS has apparent disadvantages in requiring a light source for data reading. The data retention of the SGPS may be disturbed by long-term light illumination. For example, the gate filter may change the phase from *a* to *c* due to long-term light illumination. Note that the resistance of the top gate varies by about 2 orders at the *a/c* phases. Thus, alternate operating methods requiring no light source but via the top gate resistance variations are being explored.

Table 2: Performances of the SGPS and the other memories

Devices	Graphene SGPS	Graphene switch device	Graphene NVM	Flash	MRAM	PRAM	RRAM
Device structure	Graphene FET with a switchable optical gate filter	Graphene FET	Graphene FET with a charge trapping stack	MOSFET with a charge trapping stack (1T)	A switchable resistor and a transistor (1T1R)	A chalcogenide resistor and a selector (1D1R)	A Ti/TiO ₂ /Ti resistor and a selector (1D1R)
Device size	-	-	-	4F ² (NAND)	16 - 8F ²	4F ²	4F ²
Storage mechanism	Switch of the gate filter's optical transmittance for the graphene photo-sensor	Vary the electric resistance of the graphene channel by oxidizing the channel graphene	Charge trapping induced gate potential increase	Charge trapping induced gate potential increase	Vary the electric resistance of the resistor by manipulating the electron spin	Vary the electric resistance of the resistor via phase switch of chalcogenide	Under debate
Write/read/erase speed	~50ns/10ns/50ns	80μs/?/80μs	10ms/?/30ms	~μs/60ns/~ms	30ns/30ns/30ns	10ns/50ns/20ns	80ns/μs/80ns
Program power	Low	High	High	Low	Medium	Low	Medium
10-year data retention	Very good	? days	Good	Good	Very good	Very Good	Good
P/E endurance	>10 ⁶ cycles	No less 8 cycles	-	10 ⁴ - 10 ⁵ cycles	>10 ¹² cycles	>10 ¹² cycles	10 ¹² cycles
References	This study	[4] EDL v29n8, p952, 2008.	[5] VLSI Tech. 11 t6b1, p118	[9] IEDM 2001 s36p5, p803	[9] IEDM 2001 s36p5, p803	[9] IEDM 2001 s36p5, p803	[9] IEDM 2001 s36p5, p803

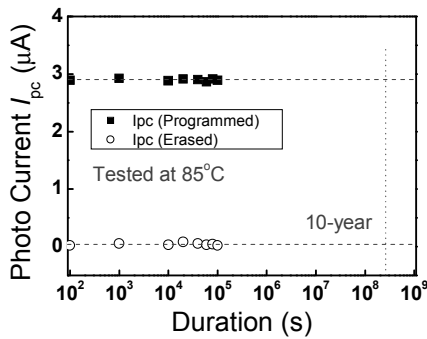


Fig. 8: Photo current I_{pc} characteristics of the SGPS at 85°C during 10⁵ s. The extrapolated 10-year retention is well demonstrated.

Fig. 8 shows good data retention for the SGPS throughout 10⁵ s at 85°C. The extrapolated 10-year data retention is very well maintained at 85°C. Note that the light source is provided only during the data reading in this study. The effects of long-term light illumination for the gate filter at the *a* phase need to be further studied.

Fig. 9 shows good cycling endurance for the SGPS by 10⁶ switching cycles between the *a/c* phases of the gate filter. The read I_{pc} remains ~3 μA throughout the 10⁶ switching cycles. It has been reported that the electric resistance of the GeSbTe is endurable throughout 10¹¹ - 10¹² switching cycles between the *a/c* phases [8]. We think that the optical transmittance of the GeSbTe may also be endurable during such a phase switching cycling. Thus, it is expected that the SGPS may show cycling endurance of 10¹¹ - 10¹² switching cycles.

With fast program/read/erase speed, non-volatility, reliable data retention and promising cycling endurance, the SGPS is likely a promising candidate for multiple functional graphene devices applications. Furthermore, as the SGPS detects the I_{pc} for data reading, it is insensitive to the disturbance induced by the very small on/off ratio (usually less than 2 orders) of the graphene field-effect transistors. Nevertheless, the SGPS may suffer from large power consumption due to not only the large I_{gt} during programming but also the large off-state current of the graphene channel.

CONCLUSION

The SGPS is demonstrated for non-volatile data storage and proposed for other potential applications. When used for non-volatile data storage, the SGPS shows promising performance in fast speed, good data retention and cycling endurance.

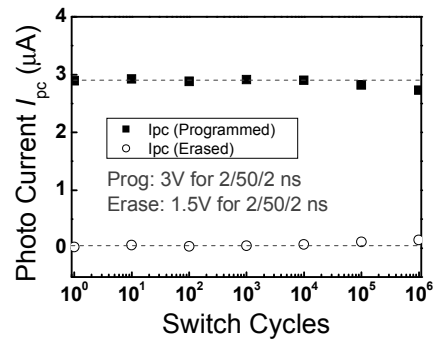


Fig. 9: Photo current I_{pc} characteristics of the SGPS throughout 10⁶ phase switching cycles. (Note that in this study, the gate filter has been cycled apart from the photo-sensor and then assembled again.)

REFERENCES

- [1] Q. Zhang et al., "Graphene nanoribbon tunnel transistors," *IEEE Electron Device Letts.*, vol. 29, no. 12, pp. 1344-1346, 2008.
- [2] Y. Wang et al., "High performance graphene FETs with self-aligned buried gates fabricated on scalable patterned Ni-catalyzed graphene," in *Symp. VLSI Tech. Dig.*, 2011, t6b1, pp. 116-117.
- [3] Ph. Avouris et al., "Graphene-based fast electronics and optoelectronics," in *IEDM Tech. Dig.*, 2010, s23p1, pp. 552-555.
- [4] T. Echtermeyer et al., "Nonvolatile switching in graphene field-effect devices," *IEEE Electron Device Letts.*, vol. 29, no. 8, pp. 952-954, 2008.
- [5] S. M. Kim et al., "Non-volatile graphene channel memory (NVGM) for flexible electronics and 3D multi-stack ultra-high-density data storages," in *Symp. VLSI Tech. Dig.*, 2011, t6b2, pp. 118-119.
- [6] M. Wuttig et al., "Phase-change materials for rewriteable data storage," *Nature Materials*, vol. 6, pp. 824-832, 2007.
- [7] M. Lankhorst et al., "Low-cost and nanoscale non-volatile memory concept for future silicon chips," *Nature Materials*, vol. 4, pp. 347-352, 2005.
- [8] I. S. Kim et al., "High performance PRAM cell scalable to sub-20nm technology with below 4F² cell size, extendable to DRAM applications," in *Symp. VLSI Tech. Dig.*, 2010, t19b3, pp. 203-204.
- [9] S. Lai et al., "OUM - A 180 nm nonvolatile memory cell element technology for stand alone and embedded applications," in *IEDM Tech. Dig.*, 2001, s36p5, pp. 803-806.